J|A|C|S COMMUNICATIONS

# Fabrication of Ordered Nanostructures of Sulfide Nanocrystal Assemblies over Self-Assembled Genetically Engineered P22 Coat Protein

Liming Shen,[†] Ningzhong Bao,[†] Peter E. Prevelige,*[,‡] and Arunava Gupta*[,†]

*Center for Materials for Information Technology, University of Alabama, Tuscaloosa, Alabama 35487, United States, and Department of Microbiology, University of Alabama at Birmingham, Birmingham, Alabama 35294, United States*

Received August 6, 2010; E-mail: prevelig@uab.edu; agupta@mint.ua.edu

***Abstract:*** Ordered ZnS and CdS nanocrystal assemblies have been synthesized by a facile bioinspired approach consisting of an initial self-assembly of engineered proteins into spherical biotemplates and a subsequent protein-directed nucleation and growth of ZnS and CdS nanocrystals symmetrically distributed over the self-assembled biotemplates.

Ordered nanoparticle assemblies are of considerable interest because of their novel collective properties and potential applications in diverse areas such as catalysis, drug delivery, biomedicine, composites, etc.[1] A major challenge in the assembly of nanoparticles lies in the development of controllable synthetic strategies that can enable growth and assembly of target nanoparticles with high selectivity and good controllability.[2] Biological systems ranging from microbes to complex multicellular systems are known to possess intrinsic recognition mechanisms for inorganic species and sophisticated self-assembly processes, as evidenced by the synthesis of linear arrays of magnetic $Fe_3O_4$ nanoparticles in magnetotactic bacteria, tough nanostructured hybrids of shells and bones in multicellular organisms, etc.[3] As a step toward mimicking some of these biological self-assembly processes, a variety of organisms have been exploited in recent years as templates for the construction of intricate nanostructures with controlled size, shape, structure, and functionality.[4]

Peptides and proteins have been quite extensively investigated during the early phase of research in biomimetic synthesis. This is primarily because of their ease of functionalization, specific recognition and interaction with diverse materials, and ability to self-assemble as exhibited in natural biomineralization processes.[5] A number of protein architectures, such as apoferritin, heat shock protein, and cowpea chlorotic mottle virus, have been studied for the growth of uniform nanoparticles including metals, semiconductors, and magnetic oxides.[6] The intrinsic nanometer-size inner cavity of such protein cages helps to spatially constrain the growth of the nanoparticles/nanocrystals and results in very good homogeneity in the resultant size and shape. In order to fabricate complex inorganic nanostructures using protein templates, more effort has been devoted to protein surface modification to enhance the binding affinity for creating interesting nanostructures of designed materials.[7] Belcher's group was one of the first to express specific peptides, screened out using a phage display library, on filamentous M13 bacteriophage for biosynthesis.[8] The results from their group and others indicate that the addition of specific peptides can greatly enhance the selectivity and binding affinity of protein templates for inorganic materials synthesis.[7,8] To date, a large number of peptides have been screened for specific binding affinity to different substrates, including metals, oxides, and semiconductors.[9] The synthesized inorganic materials include nanoparticles[8a,b] and, in particular, interesting nanostructures of nanowires and a double helical superstructure of nanoparticle assemblies over self-assembled peptides.[8c,10] Moreover, the use of self-assembling engineered proteins is promising for use as a biomimetic scaffold for achieving the rational control of ordered inorganic nanostructures with designed components and architectures.[2,11]

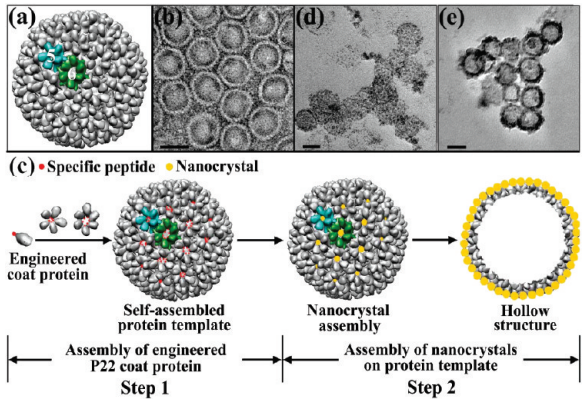


***Figure 1.*** (a) Three-dimensional surface representation of P22 procapsid viewed along a 3-fold axis. (b) TEM image of stained protein assemblies of genetically engineered P22 coat protein. (c) Schematic illustration of the formation of ordered nanocrystal assemblies over self-assembled genetically engineered P22 coat proteins. Step 1: assembly of P22 coat proteins (gray) genetically engineered with specific peptide (red). Step 2: protein-directed nucleation and growth of nanocrystals (yellow) on the protein assembly. (d and e) Sulfide nanocrystal assemblies grown on the self-assembled protein templates shown in Figure 1b. All scale bars represent 50 nm.

In this communication, we demonstrate a biotemplated construction of ordered nanocrystal assemblies using a two-step procedure: (1) the self-assembly of spherical protein templates from the genetically engineered P22 coat protein; and (2) the nucleation and growth of nanocrystals on the self-assembled protein templates. We have used ZnS and CdS grown on the engineered P22 coat protein assembly as a model system since binding peptides with strong affinity for these sulfides have been identified. Furthermore, the structure and assembly of the P22 coat proteins are reasonably well understood. The synthetic strategy is quite general and can be extended to the fabrication of a variety of other nanostructures.

Figure 1 demonstrates the formation of ordered sulfide nanocrystal assemblies over self-assembled genetically engineered P22 coat proteins. Hereafter, we refer to these hybrid structures as sulfide (ZnS or CdS) nanostructures. The assembly process and the resultant structure of protein templates are similar to those of the wild P22 procapsid. Typically, 420 copies of the P22 coat protein of MW $\approx$ 47 kDa assemble with the aid of approximately 300 copies of the

[†] University of Alabama, Tuscaloosa.
[‡] University of Alabama at Birmingham.

33.6 kDa scaffolding protein to form an icosahedral $T = 7$ P22 procapsid (Figure 1a).[12] The protein assembly (Figure 1b) has been established to have an approximate diameter of 58 nm. The structure of the protein assembly can be viewed as consisting of 60 hexamers clustered along with 12 pentamers at the vertices; one of each kind is marked by Numbers 5 and 6, respectively, in Figure 1a. Each pentamer is roughly 12.5 nm in diameter, while the axes of the slightly skewed hexamer are approximately 11 and 13 nm. Both the pentamers and hexamers contain channels of about 3 nm in diameter.[12a] In the self-assembly of the genetically engineered P22 coat protein, as shown in Figure 1c, a foreign peptide is inserted between coat protein residues 182 and 183 by PCR based mutagenesis (see details of genetic engineering of P22 coat protein in the Supporting Information (SI)). These residues lie in the middle of a flexible loop region on the protein surface such that it has the tolerance for addition of a short peptide.[12b] Peptide sequences with strong affinity for the sulfides, ZnS (CNNPMHQNC) and CdS (SLTPLTTSHLRS), have previously been identified from a phage display peptide library by Belcher's group.[8a] On the resultant protein assembly, the engineered peptides ring the central channel of each of the pentamers and hexamers as dictated by the geometrical location of the original coat protein residue 182. In a typical inorganic synthesis, the protein-directed nucleation of sulfide nanocrystals occurs at the engineered regions on the protein surface. Since the central cavity of a pentamer or hexamer is about 3 nm in diameter, it can aid in the growth of a nanocrystal from several sulfide nuclei formed over five (pentamer) or six (hexamer) fused peptides.[13] Thus, an engineered protein assembly is theoretically capable of forming 72 sulfide nanocrystals symmetrically distributed on its surface. By changing the reaction time and reactant concentration, the final protein-directed sulfide growth is expected to exhibit different structures, such as ordered spherical nanocrystal assemblies (Figure 1d) during the early stage of growth that eventually develop into spherical hollow nanostructures for longer growth periods (Figure 1e). The inner protein layer of the spherical hollow nanostructures can be eliminated by gentle heating or out-diffusion of denatured proteins without disturbing the hollow structure of the sulfide coating.[14] Experimental details are provided in the SI, and the products have been investigated using transmission electron microscopy (TEM) coupled with high resolution (HR).

In order to verify the directing function of the protein template in the nucleation and growth of ZnS, we determined the actual number of nanocrystals formed after a short reaction period on the protein template. Figure 2a shows the TEM image of two ZnS nanostructures and their nanocrystal subunits. Since the ZnS nanocrystals are discontinuously distributed over the protein assemblies and each of them can scatter the electron beam to provide contrast, the number of nanocrystals can be counted. The number of distinct nanocrystals in each nanostructure (Figure 2a) has been determined to be 65 for the one on the bottom-left (Figure 2b) and 70 for the top-right nanostructure (Figure 2c), respectively. The number of nanocrystals is very close to the predicted value of 72, the total number of pentamers and hexamers within one protein assembly. Figure 3a shows the TEM image of a spherical ZnS nanostructure grown on genetically engineered P22 coat protein assembly. The HRTEM image of a typical individual nanocrystal is provided in Figure 3b, which shows lattice fringes with a spacing of $d = 0.337 \pm 0.006$ nm, corresponding to the (100) planes of the wurtzite (hexagonal) structure of ZnS. The selected area electron diffraction (SAED) (Figure S1) pattern of the ZnS nanostructures over a large area can also be indexed to a hexagonal wurtzite structure with polycrystalline characteristics, consistent with the results reported by Belcher's group.[8a] For site-specific nucleation

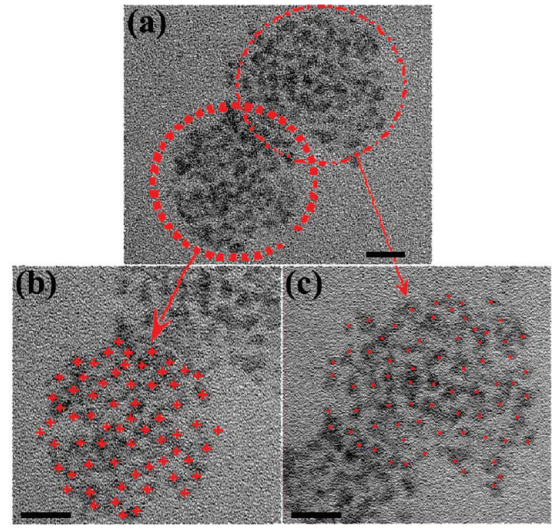


***Figure 2.*** (a) TEM image of two connected ZnS nanostructures formed after 2 h; magnified TEM images of (b) the bottom-left and (c) the top-right nanostructures shown in Figure 2a. Protein-templated nanocrystal subunits are marked in red. All scale bars represent 20 nm.

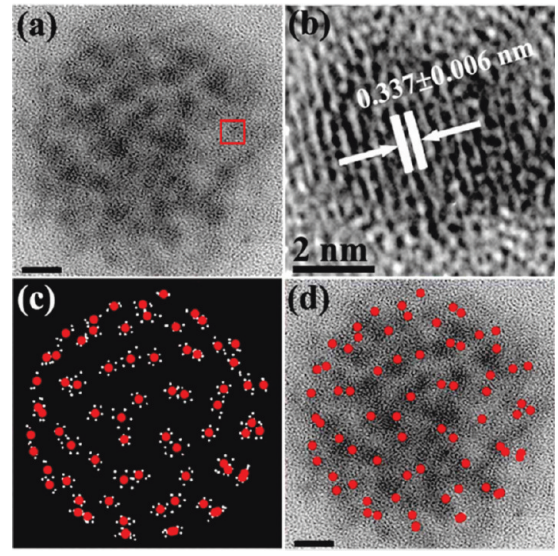


***Figure 3.*** (a) TEM image of a spherical ZnS nanostructure and (b) HRTEM image of one crystal subunit taken from the boxed area shown in Figure 3a. (c) Simulated structure of P22 coat protein assembly generated by PyMOL molecular visualization system, showing protein residue 182. The red dots indicate the center of the hexamers and pentamers. (d) Superimposed simulated structure of Figure 3c on synthesized ZnS nanostructure. The scale bar in Figure 3a and 3d represents 10 nm.

and growth of the nanocrystals the pattern of electron dense ZnS nanocrystals should correspond to the locations of the fusion peptides on the protein assembly. The particles can affix to the grid with any rotation about the Euler angles $\alpha$, $\beta$, $\gamma$, and different orientations will result in different projected patterns of the ZnS nanostructure. We have verified the ability of genetically engineered proteins to direct the construction of inorganic nanostructures by matching the locations of the synthesized ZnS nanocrystals to the location of the fusion peptides on the protein assembly. Figure 3c displays the two-dimensional projection image of the locations of the fusion peptide (small white dots) projected from the orientation providing the best match to one observed ZnS nanostructure. The 72 red dots indicate the center of the pentamers and hexamers, the expected locations for nanocrystal growth. The correspondence

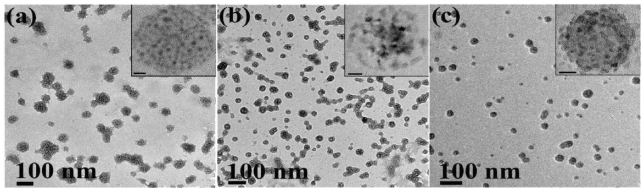


***Figure 4.*** TEM images of CdS nanostructures grown on the template of protein assemblies: (a) spherical nanoclusters of CdS quantum dots, (b) spherical CdS nanocrystal assemblies, and (c) hollow nanostructures of CdS nanocrystal assemblies. The insets to a−c are TEM images of representative individual nanostructures. All scale bars represent 10 nm.

between the projected dot pattern and the ZnS nanocrystals for one nanostructure is shown in Figure 3d. There are partial mismatches, which is likely due to the deformation of the protein template during sample preparation and TEM imaging. The correspondence between fusion peptide and nanocrystal location for a second ZnS nanostructure affixed to the grid in a different orientation is shown in Figure S2 in the SI.

We have also studied the nanopatterned assembly of CdS nanocrystals and their evolution on the surface of the self-assembled genetically engineered P22 coat protein. For this purpose, as in the case of ZnS, a peptide with specific affinity to CdS is inserted into the P22 coat protein. The size, shape, and structure of the synthesized ordered sulfide nanostructures can again be manipulated by varying the reaction time and reactant concentration. The nucleation and growth of CdS over the assembled proteins after a short reaction period result in the formation of the nanoclusters that are composed of ∼2 nm quantum dots, as shown in Figure 4a. The HRTEM image (Figure S3d) of a typical CdS nanostructure shows clear crystal lattice fringes with an interlayer spacing measured to be $0.244 \pm 0.001$ nm, very close to the lattice spacing of the (102) planes of 0.245 nm in hexagonal CdS. The SAED (Figure S4) pattern of the CdS nanostructures over a large area also indexes to the hexagonal wurtzite structure with polycrystalline characteristics. We have also investigated the dot-pattern match between the synthesized CdS nanoclusters and the location of the fusion peptides on the protein assembly (Figure S5). The good correspondence further confirms that the sulfide nanocrystals specifically nucleate at the engineered peptide sites.

By prolonging the reaction time, each CdS quantum dot subunit within the initially formed nanoclusters grows larger to form ordered assemblies of more densely packed nanocrystals while still maintaining the nanocluster structure (Figure 4b). With increasing both the reaction time and reactant concentration, the nanoclusters evolve into spherical hollow nanostructures (Figure 4c), accompanying the continued growth of the CdS quantum dot subunits to ∼5 nm that essentially covers a major fraction of the protein template surface. All these nanostructures can form monodisperse layers on a large scale (Figures S3, S6−S7). A similar nanostructure evolution has also been observed for ZnS nanocrystal assemblies on engineered P22 coat protein templates (Figures S8−S9). We finally note that only the genetically engineered P22 coat protein assemblies serve as efficient templates for the protein-directed nucleation and growth of the unique sulfide nanostructures. Nonspherical nanoparticle agglomerates are obtained in the presence of wild P22 capsids (Figure S10a), protein assemblies engineered with a nonspecific peptide (Figure S10b), and in the absence of any protein template (Figure S10c).

Both the diameter and configuration of the self-assembled P22 coat protein template can be tuned over a limited range by heating in solution at temperatures of up to 70 °C.[15] This potentially offers some degree of control over the size and shape of the synthesized inorganic nanostructures. Additionally, the crystallite size of the nanocrystals can be varied by changing the reactant concentration and the reaction time.[16] A relatively high reactant concentration and longer reaction time can result in the formation of large sulfide nanocrystals due to their very low solubility product constants. In this study, we obtained sulfide nanocrystals in the size range of 2−5 nm using low concentrations of reactants.

In summary, we have demonstrated a controllable approach for the construction of ordered ZnS and CdS nanostructures over genetically engineered P22 coat protein assemblies. The high-affinity ZnS- and CdS-binding peptides, identified from a phage display library, enable the selective nucleation and growth of sulfides over the complex protein assemblies. The demonstrated strategy can be expanded to serve as a general bioinspired approach for the design of nanoparticle assemblies with desired components and architectures.

**Acknowledgment.** This research was supported by the U.S. Department of Energy, Office of Basic Energy Sciences, Division of Materials Sciences and Engineering under Award No. DE-FG02-08ER46537.

**Supporting Information Available:** Experimental details and additional supporting TEM images. This material is available free of charge via the Internet at http://pubs.acs.org.

## References

(1) (a) Zhou, S.; McIlwrath, K.; Jackson, G.; Eichhorn, B. *J. Am. Chem. Soc.* **2006**, *128*, 1780–1781. (b) Cheng, K.; Peng, S.; Xu, C.; Sun, S. *J. Am. Chem. Soc.* **2009**, *131*, 10637–10644. (c) Xu, C.; Wang, B.; Sun, S. *J. Am. Chem. Soc.* **2009**, *131*, 4216–4217. (d) Choi, S.-H.; Na, H. B.; Park, Y.; An, K.; Kwon, S. G.; Jang, Y.; Park, M.; Moon, J.; Son, J. S.; Song, I. C.; Moon, W. K.; Hyeon, T. *J. Am. Chem. Soc.* **2008**, *130*, 15573–15580. (e) Ge, J.; Hu, Y.; Yin, Y. *Angew. Chem., Int. Ed.* **2007**, *46*, 7428–7431.

(2) (a) Nie, Z.; Petukhova, A.; Kumacheva1, E. *Nat. Nanotechnol.* **2010**, *5*, 15–25. (b) Glotzer, S. C.; Solomon, M. J. *Nat. Mater.* **2007**, *6*, 557–562.

(3) (a) Sarikaya, M.; Tamerler, C.; Jen, A.-Y.; Schulten, K.; Baneyx, F. *Nat. Mater.* **2003**, *2*, 577–585. (b) Sanchez, C.; Arribart, H.; Guille, M. M. G. *Nat. Mater.* **2005**, *4*, 277–288.

(4) (a) Douglas, T.; Young, M. *Science* **2006**, *312*, 873–875. (b) Palmer, L. C.; Stupp, S. I. *Acc. Chem. Res.* **2008**, *41*, 1674–1684. (c) Cheung, C. L.; Chung, S.; Chatterji, A.; Lin, T.; Johnson, J. E.; Hok, S.; Perkins, J.; De Yoreo, J. J. *J. Am. Chem. Soc.* **2006**, *128*, 10801–10807. (d) Crookes-Goodson, W. J.; Slocik, J. M.; Naik, R. R. *Chem. Soc. Rev.* **2008**, *37*, 2403–2412.

(5) (a) Zhang, S. *Nat. Biotechnol.* **2003**, *21*, 1171–1178. (b) Chen, C.; Rosi, N. L. *Angew. Chem., Int. Ed.* **2010**, *49*, 1924–1942.

(6) (a) Varpness, Z.; Peters, J. W.; Young, M.; Douglas, T. *Nano Lett.* **2005**, *5*, 2306–2309. (b) Ueno, T.; Suzuki, M.; Goto, T.; Matsumoto, T.; Nagayama, K.; Watanabe, Y. *Angew. Chem., Int. Ed.* **2004**, *43*, 2527–2530. (c) Ensign, D.; Young, M.; Douglas, T. *Inorg. Chem.* **2004**, *43*, 3441–3446. (d) Kramer, R. M.; Li, C.; Carter, D. C.; Stone, M. O.; Naik, R. R. *J. Am. Chem. Soc.* **2004**, *126*, 13282–13286. (e) Iwahori, K.; Enomoto, T.; Furusho, H.; Miura, A.; Nishio, K.; Mishima, Y.; Yamashita, I. *Chem. Mater.* **2007**, *19*, 3105–3111. (f) Klem, M. T.; Resnick, D. A.; Gilmore, K.; Young, M.; Idzerda, Y. U.; Douglas, T. *J. Am. Chem. Soc.* **2007**, *129*, 197–201. (g) Klem, M. T.; Willits, D.; Young, M.; Douglas, T. *J. Am. Chem. Soc.* **2003**, *125*, 10806–10807.

(7) (a) Flenniken, M. L.; Liepold, L. O.; Crowley, B. E.; Willits, D. A.; Young, M. J.; Douglas, T. *Chem. Commun.* **2005**, *447*, 449. (b) Uchida, M.; Flenniken, M. L.; Allen, M.; Willits, D. A.; Crowley, B. E.; Brumfield, S.; Willis, A. F.; Jackiw, L.; Jutila, M.; Young, M. J.; Douglas, T. *J. Am. Chem. Soc.* **2006**, *128*, 16626–16633.

(8) (a) Flynn, C. E.; Mao, C.; Hayhurst, A.; Williams, J. L.; Georgiou, G.; Iversona, B.; Belcher, A. M. *J. Mater. Chem.* **2003**, *13*, 2414–2421. (b) Whaley, S. R.; English, D. S.; Hu, E. L.; Barbara, P. F.; Belcher, A. M. *Nature* **2000**, *405*, 665–668. (c) Mao, C.; Solis, D. J.; Reiss, B. D.; Kottmann, S. T.; Sweeney, R. Y.; Hayhurst, A.; Georgiou, G.; Iverson, B.; Belcher, A. M. *Science* **2004**, *303*, 213–217.

(9) (a) Li, Y.; Whyburn, G. P.; Huang, Y. *J. Am. Chem. Soc.* **2009**, *131*, 15998–15999. (b) Khoo, X.; Hamilton, P.; O'Toole, G. A.; Snyder, B. D.; Kenan, D. J.; Grinstaff, M. W. *J. Am. Chem. Soc.* **2009**, *131*, 10992–10997. (c) Heinz, H.; Farmer, B. L.; Pandey, R. B.; Slocik, J. M.; Patnaik, S. S.; Pachter, R.; Naik, R. R. *J. Am. Chem. Soc.* **2009**, *131*, 9704–9714. (d) Sano, K.; Shiba, K. *J. Am. Chem. Soc.* **2003**, *125*, 14234–14235. (e) Zhou, W.; Schwartz, D. T.; Baneyx, F. *J. Am. Chem. Soc.* **2010**, *132*, 4731–4738. (f) Roach, P.; Farrar, D.; Perry, C. C. *J. Am. Chem. Soc.* **2005**, *127*, 8168–8173. (g) Zorbas, V.; Smith, A.; Xie, H.; Ortiz-Acevedo, A.; Dalton, A. B.; Dieckmann, G. R.; Draper, R. K.; Baughman, R. H.; Musselman, I. H. *J. Am. Chem. Soc.* **2005**, *127*, 12323–12328. (h) Banerjee, I. A.; Yu, L.; Matsui, H. *J. Am. Chem. Soc.* **2005**, *127*, 16002–16003.

(10) (a) Chen, C. L.; Rosi, N. L. *J. Am. Chem. Soc.* **2010**, *132*, 6902–6903. (b) Chen, C. L.; Zhang, P. J.; Rosi, N. L. *J. Am. Chem. Soc.* **2008**, *130*, 13555–13557.
(11) (a) Chen, C. L.; Rosi, N. L. *Angew. Chem., Int. Ed.* **2010**, *49*, 1924–1942. (b) Stephanopoulos, N.; Liu, M.; Tong, G. Y.; Li, Z.; Liu, Y.; Yan, H.; Francis, M. B. *Nano Lett.* **2010**, *10*, 2714–2720.
(12) (a) Thuman-Commike, P. A.; Greene, B.; Jakana, J.; Prasad, B. B. V.; King, J.; Prevelige, P. E.; Chiu, W. *J. Mol. Biol.* **1996**, *260*, 85–98. (b) Kang, S.; Lander, G. C.; Johnson, J. E.; Prevelige, P. E. *ChemBioChem* **2008**, *9*, 514–518. (c) Lander, G. C.; Tang, L.; Casjens, S. R.; Gilcrease, E. B.; Prevelige, P. E.; Poliakov, A.; Potter, C. S.; Carragher, B.; Johnson, J. E. *Science* **2006**, *312*, 1791–1795.
(13) (a) Zheng, H.; Smith, R. K.; Jun, Y.; Kisielowski, C.; Dahmen, U.; Alivisatos, A. P. *Science* **2009**, *324*, 1309–1312. (b) Privman, V.; Goia, D. V.; Park, J.; Matijevic, E. *J. Colloid Interface Sci.* **1999**, *213*, 36–45. (c) Bao, N.; Shen, L.; Wang, Y.-H. A.; Ma, J.; Mazumdar, D.; Gupta, A. *J. Am. Chem. Soc.* **2009**, *131*, 12900–12901.
(14) (a) Lou, X. W.; Archer, L. A.; Yang, Z. *Adv. Mater.* **2008**, *20*, 3987–4019. (b) Shen, L.; Bao, N.; Prevelige, P. E.; Gupta, A. *J. Phys. Chem. C* **2010**, *114*, 2551–2559. (c) Reches, M.; Gazit, E. *Science* **2003**, *300*, 625–627.
(15) Teschke, C. M.; McGough, A.; Thuman-Commike, P. A. *Biophys. J.* **2003**, *84*, 2585–2592.
(16) (a) El-Sayed, M. A. *Acc. Chem. Res.* **2004**, *37*, 326–333. (b) Yin, Y.; Alivisatos, A. P. *Nature* **2005**, *437*, 664–670. (c) Trindade, T.; O'Brien, P.; Pickett, N. L. *Chem. Mater.* **2001**, *13*, 3843–3858. (d) Bao, N.; Shen, L.; An, W.; Padhan, P.; Turner, C. H.; Gupta, A. *Chem. Mater.* **2009**, *21*, 3458–33468. (e) Kwon, S. G.; Piao, Y.; Park, J.; Angappane, S.; Jo, Y.; Hwang, N. M.; Park, J. G.; Hyeon, T. *J. Am. Chem. Soc.* **2007**, *129*, 12571–12584.

JA107080B